J Bionic Eng 17 (2020) 959–969
DOI: https://doi.org/10.1007/s42235-020-0087-3

Journal of Bionic Engineering
http://www.springer.com/journal/42235

A Fuzzy PID Algorithm for a Novel Miniature Spherical Robots with Three-dimensional Underwater Motion Control

Liwei Shi[1*], Yao Hu[1], Shuxiang Su[1], Shuxiang Guo[1,2], Huiming Xing[1], Xihuan Hou[1], Yu Liu[1], Zhan Chen[1], Zan Li[1], Debin Xia[1]

1. *Key Laboratory of Convergence Medical Engineering System and Healthcare Technology*, *the Ministry of Industry and Information Technology*, *School of Life Science*, *Beijing Institute of Technology*, *Beijing* 100081, *China*
2. *Faculty of Engineering*, *Kagawa University*, 2217-20 *Hayashicho*, *Takamatsu*, *Kagawa* 761-0396, *Japan*

Abstract

We proposed and developed a small bionic amphibious spherical robot system for tasks such as coastal environment monitoring and offshore autonomous search and rescue. Our third-generation bionic small amphibious spherical robots have many disadvantages, such as the lack of maneuverability and a small operating range. It is difficult to accomplish underwater autonomous motion control with these robots. Therefore, we proposed a fourth-generation amphibious spherical robot. However, the amphibious spherical robot developed in this project has a small and compact design, with limited sensors and external sensing options. This means that the robot has weak external information collection capabilities. We need to make the real time operation of the robot's underwater motion control system more reliable. In this paper, we mainly used a fuzzy Proportional-Integral-Derivative (PID) control algorithm to design an underwater motion control system for a novel robot. Moreover, we compared PID with fuzzy PID control methods by carrying out experiments on heading and turning bow motions to verify that the fuzzy PID is more robust and exhibits good dynamic performance. We also carried out experiments on the three-dimensional (3D) motion control to validate the design of the underwater motion control system.

Keywords: bionic amphibious spherical robot, fuzzy PID control, underwater motion control system, underwater three-dimensional motion, water-jet thruster

1 Introduction

Amphibious robots have developed rapidly since first appearing. Such robots can be used to accomplish many types of missions, such as maritime search and rescue, monitoring of coastal transitional and marine biological environments, and long-term monitoring of marine organisms[1]]. To accomplish a variety of missions, excellent motion control is required for these robots[2–4]. The motion control of amphibious robots requires very wide-ranging knowledge, which is the key to the multidisciplinary research necessary for developing this type of robot technology. For example, dynamics calculations, path planning, optimal control, information fusion, vision, communication and navigation skills are required. The main difficulty with respect to the underwater motion control of amphibious robots is that the robot works underwater, where disturbances in the water and the influence of various uncertainties make it difficult to build a motion control systems for robots[5–7].

Nature's evolution has introduced highly efficient biological functions and mechanisms. Using this approach, a number of new application areas have recently received significant interests in the robotics community[8–12]. Recently, many researchers have focused on amphibious robots. For example, Case Western Reserve University and Naval Postgraduate School designed the Whegs series in the shape of a cymbal. Amphibious robots can adapt to all terrains[13,14]. Tokyo Institute of Technology designed an amphibious snake-shaped robot named ACM-R5[15], which features a multi-joint modular design with the same structure for each joint and a separate control unit for movement on land and in water. However, the robot is not able to achieve autonomous movement in water. An amphibious autonomous robot, AQUA, was proposed[5,16]. Rotundus AB designed an amphibious

***Corresponding author:** Liwei Shi
E-mail: shiliwei@bit.edu.cn

spherical robot named Groundbot, which was proposed as an alternative design for a Mars rover. Groundbot is driven by a pendulum and is capable of navigating rough outdoor terrains at speeds of up to 3 $m \cdot s^{-1}$ and climbing slopes of up to 15° – 18°[17]. Ye *et al*. developed an amphibious spherical robot called BYSQ, and a motion control system with visual feedback is proposed[18]. Yin *et al*. developed an amphibious robot named Chigon. The robot uses Central Pattern Generator (CPG) to generate gait control signals and ADAMS simulation software to analyze the characteristics of the motion of the robot, and model and optimize its structure[19]. A salamander-like amphibious robot named Salamandra Robotica I and its improved model named Salamandra Robotica II were designed[20]. The robot simulates the motion mechanism of the salamander and uses CPG control algorithm for motion control. However, the robot cannot achieve flexible movement in the water[20,21]. Ding *et al*. developed a multimodal amphibious robot[22]. Zhang *et al*. developed an amphibian robot named AmphiHex-I[23]. Cui *et al*. proposed and designed an amphibious robot called AmBot, which was used to monitor the ecology of the Swan-Canning estuary[24]. Vogel *et al*. developed an amphibious robot named RoboTerp[25]. Kim *et al*. developed a six-legged amphibious robot that simulates a caterpillar lizard[26,27]. Scaradozzi *et al*. proposed a hybrid propulsion underwater research vehicle[28].

In the case of underwater spherical robots: Manchester University (UK) developed two underwater spherical robots named MK-V and MK-VI. This series of robots is mainly used to monitor nuclear storage tanks and sewage treatment equipment. After implementing step-by-step updates and improvements to the mechanical design of these robots, the robot team instigated related research designed to improve the motion control of underwater spherical robots[29,30]. Kaznov *et al*. developed an amphibious spherical robot named GroundBot[31]. Satria *et al*. developed an amphibian spherical robot named Salamander[32]. Guo *et al*. developed an underwater spherical robot named SUR-II. The robot performs underwater vector water-jet propulsion through three water jet motors and is equipped with a microelectromechanical systems (MEMS) sensor, a pressure sensor and so on. The speed of the underwater movement is 0.4 $m \cdot s^{-1}$, and zero-radius rotation can be realized[33,34]. In our previous studies[35–42], an amphibious spherical robot was developed.

The above-mentioned robots all have the shortcomings of not being able to move freely on both land and water. There is no barrier to walking on land, which is not equivalent to any motion in water; underwater motion remains challenging. Most of these robots have low autonomy and most use remote controls, or are still being simulated. Therefore, we developed an amphibious spherical robot with high mobility, concealment, and adaptability, among other advantages. We adopted a hybrid drive mechanism to accomplish motion control in the amphibious environment. The hybrid drive mechanism includes mechanical legs and water-jet thrusters. There are various control algorithms for robots. Common ones are CPG, PID control, fuzzy control, neural network control, adaptive control, and sliding mode control. The control algorithm of existing works analyzed the dynamic and kinematic models to specify transitions from one steady-state motion to another. However, the subjects of all of these studies were either amphibious robots that were not spherical, or amphibious spherical robots that move by rolling. Thus, we cannot use any of the proposed control strategies with our amphibious spherical robot because it is driven by a compound drive mechanism with both legs and water-jets.

Then, we developed an amphibious spherical robot, named robot III. The structure of the robot is shown in Fig. 1a. The mechanical structure of the robot has many disadvantages, such as insufficient underwater thrust, slow movement speed, poor waterproof performance, wireless control limited to the surface of the water, low control precision, and lack of capacity for 3D motion control underwater. For example, the thrust of the water-jet thruster is only 83 mN, and the maximum speed of the robot is only 0.1 $m \cdot s^{-1}$. It is difficult to realize an underwater motion control system if we use this type of thruster with a small thrust. The maximum dive depth of the robot is 3 m. We adopted a wireless debugging method, but this cannot be used underwater. The underwater camera depth (depth of sight) of the third-generation robot can only be measured to within

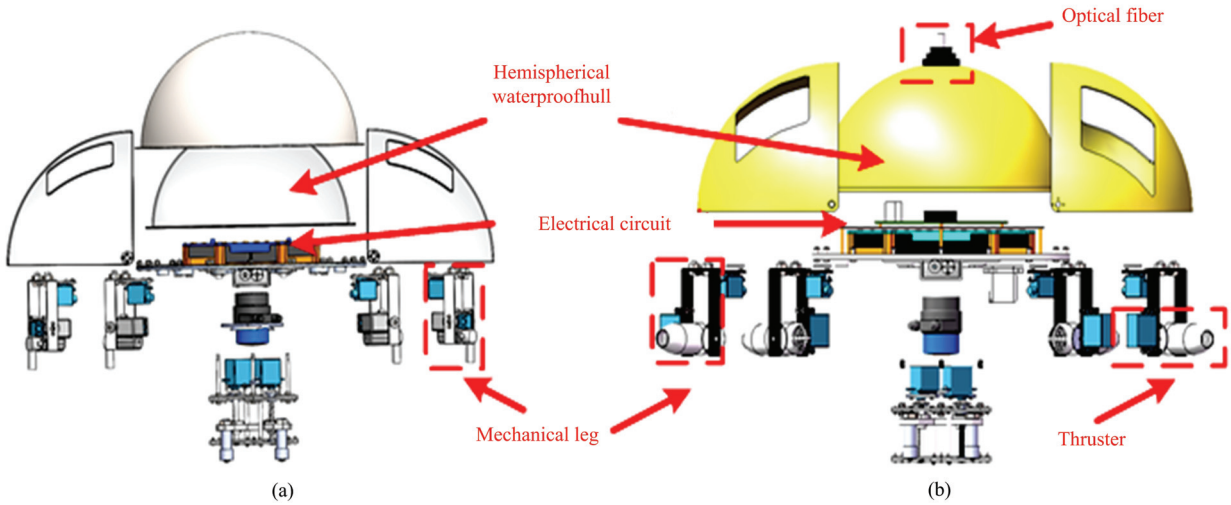

Fig. 1 Amphibious spherical robot. (a) Amphibious spherical robot III; (b) amphibious spherical robot IV.

0.5 m and the working range is small. The third-generation robot hardware circuit control system has serious heat dissipation issues, high power consumption, a lack of strong electrical isolation, and wireless signal instability.

The robot III adopted PID controller to implement walking motion on land and yawing motion in water. However, the yawing angle error is very large, and the robot can only implement one DOF motion in water by adopting PID controller. To solve the above problems, in this paper, we improve the mechanical structure and debugging method with robot IV, design fuzzy PID controllers, and implement 3D underwater motion.

The remainder of this paper is organized as follows: in section **2**, we describe our advanced robot design, the wheel-legged water-jet composite driving mechanism, and the electrical system for delivering either strong or weak power. In section **3**, we present and simplify kinematic models of the robot, using the results of thrust experiments with a water-jet thruster as a reference for the robot's vector control. In section **4**, we introduce the principle of fuzzy PID and explain how to design fuzzy PID controllers. In section **5**, we describe our forward motion, heading angle control, and depth determination experiments. The underwater 3D experiments enabled us to verify that the designed algorithm is a good solution for underwater 3D motion control. We conclude the paper in section **6**.

2 The new generation robot and control method

2.1 The mechanism

To solve some problems of current amphibious robots and robot III, we aimed to optimize the mechanical structure of robot III. We designed a new water-jet thruster with a maximum thrust of approximately 2 N, and the maximum speed increased to 1 $m \cdot s^{-1}$. We also used Acrylonitrile-Butadiene-Styrene (ABS) in the design of the spherical shell. The maximum dive depth of the robot was increased to 10 m. We also used an optical fiber plug and cables to implement communication between the robot and the ground station, allowing us to debug the robot when underwater. The fourth-generation robot uses a binocular camera, which can determine the 3D spatial position information of objects to within 5 m in the land field of view and measure over a wider range. The structural explosion diagram of robot IV is shown in Fig. 1b.

A significant feature of our robot is the hybrid drive system, as shown in Fig. 2. The robot has four legs, and each leg had two servos and one water-jet thruster. The robot can walk on land with these legs, and can swim underwater using the water-jet thruster.

2.2 The electronic circuit

The hardware circuit system of the third-generation robot also has many disadvantages. For example, the

circuit radiates significant heat, and does not allow for the collection of depth information. We improved the underwater motion control system by upgrading the hardware circuitry and mechanical structure. In the case of the hardware circuit, we used strong and weak electrical isolation to ensure safety of the robot's circuitry. We used a high-precision depth sensor so that we could control the depth of the robot, *etc*. As a power supply, the amphibious spherical robot IV contains three batteries, one of which provides power to the control center and sensor. The other two batteries provide power to the servos and thrusters. We used a TK1 (Nvidia) for the robot control center. The TK1 can receive data directly from the camera and hydrophone. However, the TK1 does not have interfaces for its depth sensors, or for control of the warning Light-Emitting Diode (LED). To receive data from the depth sensors and control the warning LED, we used a middle control board – STM32F103. The TK1 can communicate with the STM32 *via* a USB to UART module. The servo control board is controlled by the TK1 *via* the UART, and can receive commands from the TK1 and send instructions to the servos and thrusters. In this way, the robot can walk on land or swim in water. The entire electronic circuit can be described intuitively, as shown in Fig. 3.

2.3 Kinetics analysis

To fabricate a 3-D underwater motion control system, it is necessary to fully understand the kinetics of the robot. We focus on practical applications, not the derivation of mathematical formulas, in this paper. The kinetic model of the robot consists of rigid body forces and their moments, as well as hydrodynamic forces and their moments. If the underwater environment is stationary, then the kinematic equation can be written as:

$$\begin{aligned}\boldsymbol{\tau} = (\boldsymbol{M}_{\mathrm{RB}} + \boldsymbol{M}_{A})\dot{v} + \left(\boldsymbol{C}_{\mathrm{RB}}(v) + \boldsymbol{C}_{\mathrm{A}}(v)\right)v + \\ \left(\boldsymbol{D}_{\mathrm{l}} + \boldsymbol{D}_{\mathrm{q}}(v)\right)v + g(\Theta),\end{aligned} \tag{1}$$

where $\boldsymbol{M}_{\mathrm{RB}}$ is the mass matrix, $\boldsymbol{M}_{\mathrm{A}}$ is the additional mass matrix, $\boldsymbol{C}_{\mathrm{RB}}(v)$ is the Coriolis force matrix, $\boldsymbol{C}_{\mathrm{A}}(v)$ is the Coriolis matrix, $\boldsymbol{D}_{\mathrm{l}}$ is the linear damping matrix, $\boldsymbol{D}_{\mathrm{q}}(v)$ is the nonlinear damping matrix, $\boldsymbol{g}(\Theta)$ is the restoring force and moment, and $\boldsymbol{\tau}$ is the control vector.

From this model, it is clear that the robot is a nonlinear system. The most commonly used PID algorithm cannot meet our accuracy requirements, which need to take the underwater motion of the robot into account.

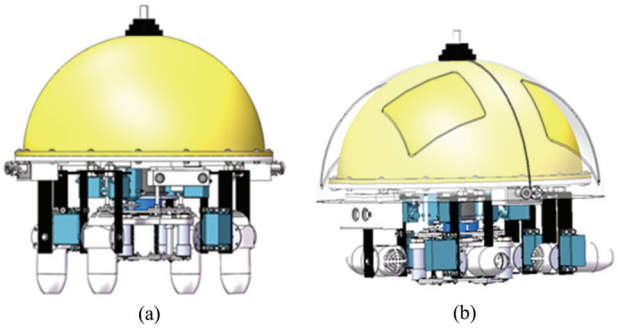

Fig. 2 The motion mode of amphibious spherical robot IV. (a) Land mode; (b) underwater mode.

2.4 Fuzzy PID

We can see from **2.3** that the kinetics model of the robot is nonlinear. Traditional control method such as PID cannot be applied to these kinds of system. However, intelligent control methods, such as neural networks, have some disadvantages, such as slow convergence and long training times. If we waste too many resources on controlling the robot, then we will not have enough resources for the visual system, because image processing requires a lot of time and resources. Hence, we need a control method that is appropriate for a nonlinear system, but has good real-time and reliability properties. The fuzzy PID control method has good robustness in nonlinear systems, as well as good real-time and reliability properties. A block diagram of a fuzzy PID control system is shown in Fig. 4.

A fuzzy PID controller involves the following processes: First, it fuzzifies the system input; then, we obtain the PID offset by fuzzy inference and defuzzification, and update the PID parameters; finally the actuator is operated through the PID controller.

3 Experiments

3.1 Land motion experiments

In the closed loop control of the robot's land motion, the heading angle obtained by the JY901 module is used as feedback. When there is an error in the direction of motion, the robot needs to adjust the heading direction through the steps of the mechanical legs on both sides.

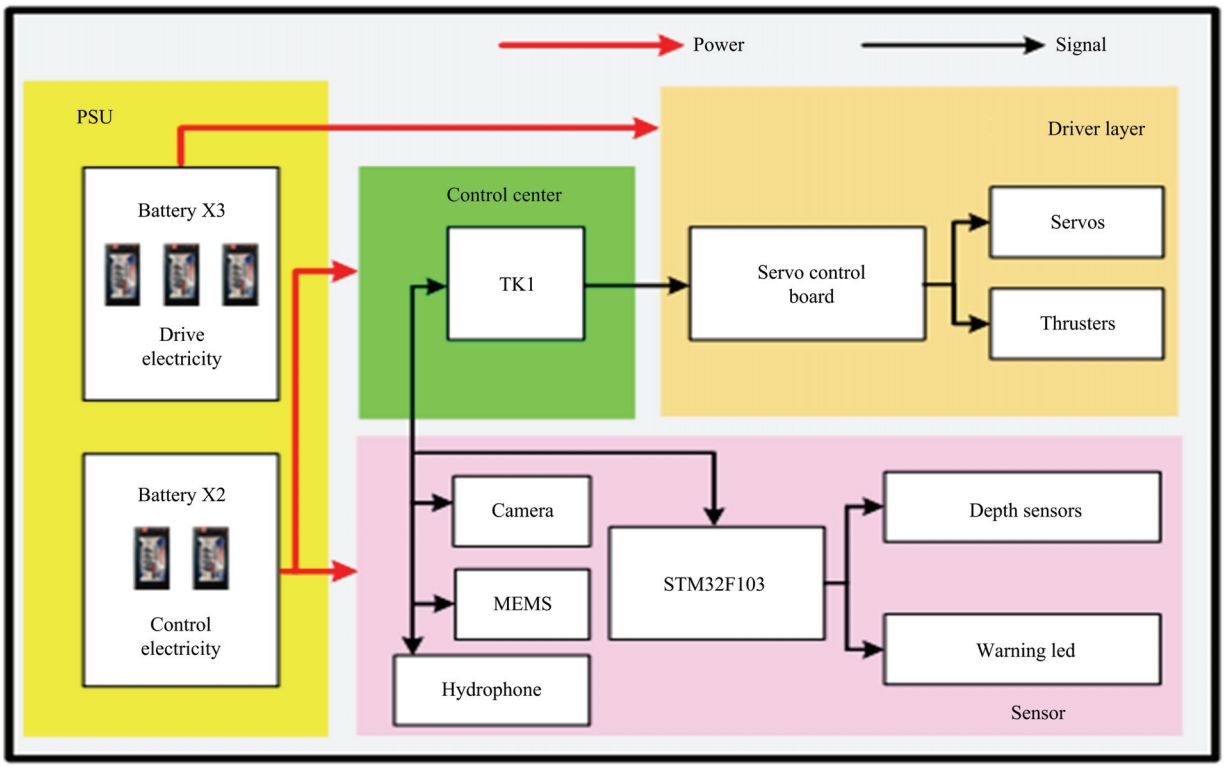

Fig. 3 The motion of amphibious spherical robot IV.

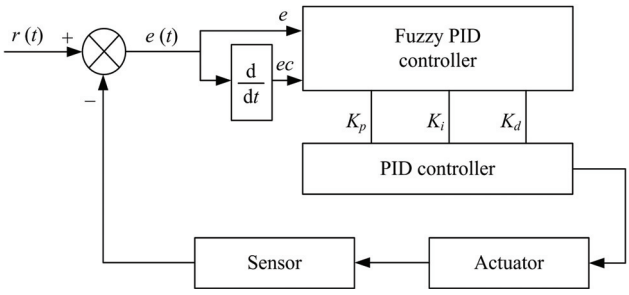

Fig. 4 Block diagram of a fuzzy PID controller.

Fig. 5 shows the experimental results of amphibious spherical robot III. In the experiment of tracking the heading position, the four red asterisks "☆" are the four heading points, and the blue line is the reference track. The positioning system based on the global camera records the trajectory of the robot. Through the analysis of robot tracking results, the maximum deviations of closed-loop PID tracking and open-loop control tracking are 7 cm and 10 cm, respectively, and the average deviations are 3.42 cm and 4.16 cm. Compared with the open-loop trajectory results, the maximum deviation and average deviation of PID closed-loop tracking decreased by 30% and 17.9%, respectively.

3.2 Forward motion experiment in water

In this section, we use the example of the amphibious spherical robot IV undergoing underwater forward motion to introduce the basic principles of the fuzzy PID control method. First, the robot collects MEMS sensor data and the robot's real-time heading angle, ψ_i, is obtained. Then we subtract the setpoint value, ψ_s, from the current heading angle ψ_i to obtain the input error value, ei, and then subtract the previous error value, e_{i-1}, from the current error, e_i. Hence, we obtain the current error change, Δe_i, the error, e_i, and the variation in the error, Δe_i, and use these values as the input to the fuzzy PID controller. After the fuzzy PID controller completes its calculation, we obtain the control quantities for the four water spray motors, which specify how to vary the spray from the four water spray motors. The water speed value controls the direction of the movement of the robot through the vector spray of the four water spray motors. Other types of motion that are similar to the forward motion are not described here. First, we carried out a forward motion experiment with our amphibious spherical robot, controlled with a fuzzy PID control algorithm in a static water tank in the labo-

ratory, and used the motion control system to advance the robot by about 2 m in the pool. As shown in Fig. 6, we ensured the accuracy of the experimental results by repeating the forward motion experiment more than 15 times and averaging the final experimental results. Figs. 6a – 6d show the forward motion experiment. Each image is from a video of the robot. The video was recorded by a camera installed above the pool. In the figure, the red line represents the direction of the robot's motion, which is also the direction of its head. We can see from Fig. 6 that the robot moves about 2 m between Fig. 6a and Fig. 6d, which takes about 15 s. Fig. 6 shows the results of the forward motion experiment, with the motion controlled by the PID controller. Fig. 7 shows the robot's forward motion when controlled by a fuzzy PID controller.

Fig. 8 shows the relationship between the forward movement of the robot and the heading angle, based on the fuzzy PID control algorithm and the PID control algorithm.

Compared with Groundbot robot and AQUA robot, these two amphibious robots adopted open loop control, which could not implement high precision of motion control. The robot III adopted PID controller to implement walking motion on land and yawing motion in water. So, we compare the experimental results of the fuzzy PID control algorithm to the PID control algorithm. When the robot moves forward in a straight line, the maximum error of the PID control algorithm is approximately 8.45°, while the maximum error of the fuzzy PID control algorithm is approximately 2.65°. From Fig. 8, we can see that the PID control algorithm slowly converges to the desired value. Though it is not good to converge to the desired the value, the convergence speed of the fuzzy PID control algorithm is fast, and the error remains small. We can also see that the fuzzy PID control algorithm performs better than the PID control algorithm, with less error. In addition, we also compute the mean square errors in the forward motion experiments. The mean square error is 0.8884° for the fuzzy PID control algorithm in this paper, while that is 10.8607° for the PID algorithms.

3.3 Turn bow motion experiment

In an experiment on the transition motion of the amphibious spherical robot, first, the robot heads straight for 80 cm, then turns 90° and heads straight

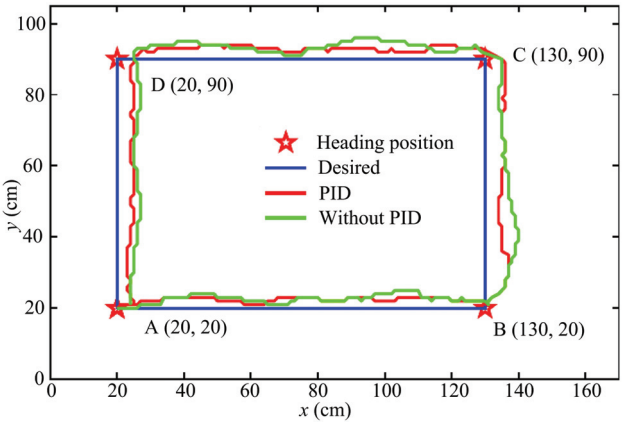

Fig. 5 The performance of the PID algorithm in the land motion experiments.

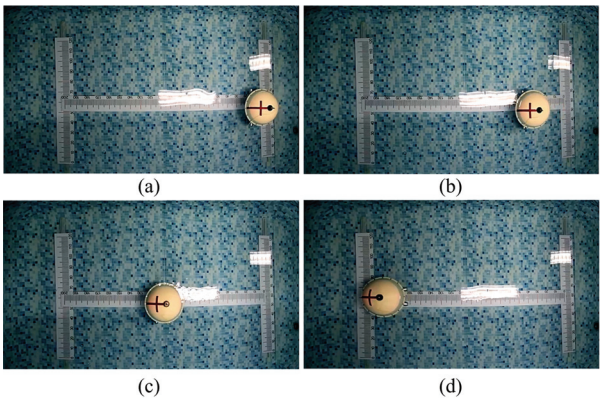

Fig. 6 PID-based forward motion experiment. (a) 0 s; (b) 5 s; (c) 10 s; (d) 15 s.

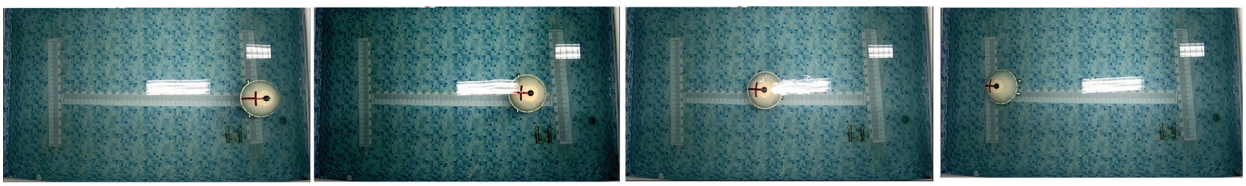

Fig. 7 Fuzzy- PID-based forward motion experiment in water. (a) 0 s; (b) 5 s; (c) 10 s; (d) 15 s.

again, for another 120 cm. Fig. 9 shows the results of the PID-based transition motion experiment. To ensure the accuracy of the experimental results, we repeated the transitional motion experiment more than 15 times and averaged the results. Figs. 9a – 9d show the results of the transition experiments. Each picture shows the motion of the robot at different times. We can see from Fig. 9 that the robot completes the transition motions shown in Figs. 9a – 9d in about 16 s. Fig. 10 shows the robot's forward motion when controlled using the fuzzy PID controller.

Fig. 11 shows the relationship between the rectangular motion of the robot and the experimental time-heading angle diagram when controlled by the fuzzy PID control algorithm and the PID control algorithm under hydrostatic conditions. As shown in Fig. 11, the robot adopts the rise time of the PID control algorithm during the transitional motion; the rise time of the fuzzy PID control algorithm is equal to the peak times of the standard and fuzzy PID control algorithms. Fig. 11 shows that the speed of the PID control algorithm converges slowly to the expected value. However, the convergence speed of the fuzzy PID control algorithm is fast, and remains close to the expected value. The peak value of the fuzzy PID algorithm is larger than that of the standard PID algorithm. However, the fuzzy PID algorithm responds and converges quickly. The fuzzy PID controller is already stable by the time that the PID algorithm reaches its peak. We can see that the fuzzy PID control algorithm performs better than the PID control algorithm even when the error is large, and the fuzzy PID control algorithm has better dynamic performance than the PID control algorithm.

3.4 3D motion experiment

We carried out a 3D underwater motion experiment with the amphibious spherical robot: We allowed the robot to travel in a straight line at a certain depth, then let the robot turn through a right angle. Once the robot reached a desired position, we moved it down towards a specified depth range to complete the experiment. Fig. 12 shows the results of the underwater 3D motion experiment when controlling the robot with the fuzzy PID algorithm. We ensured the accuracy of the experimental results by repeating the experiment more than 15 times and averaging the data. Figs. 12a – 12i show the results of these experiments. Each picture shows the motion of the robot at different times. We can see from Fig. 12 that

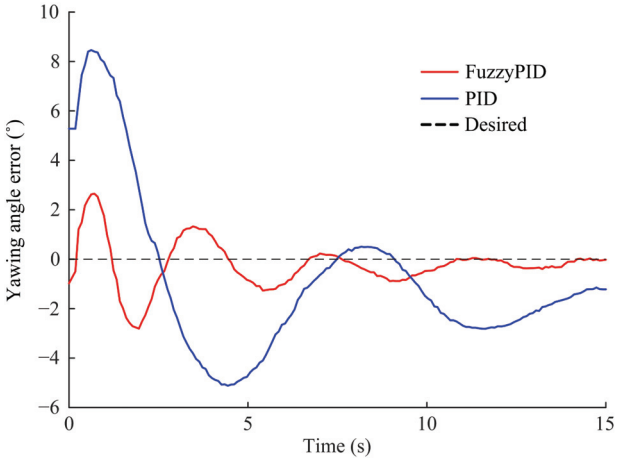

Fig. 8 Comparison between the performance of the fuzzy PID and PID algorithms in the forward motion experiments.

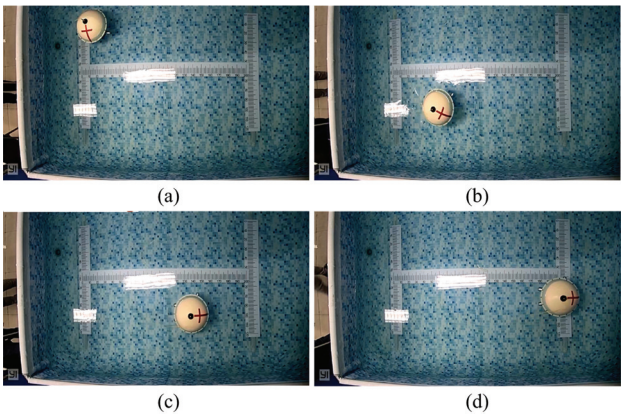

Fig. 9 PID-based turn bow motion experiment. (a) 0 s; (b) 8 s; (c) 12 s; (d) 16 s.

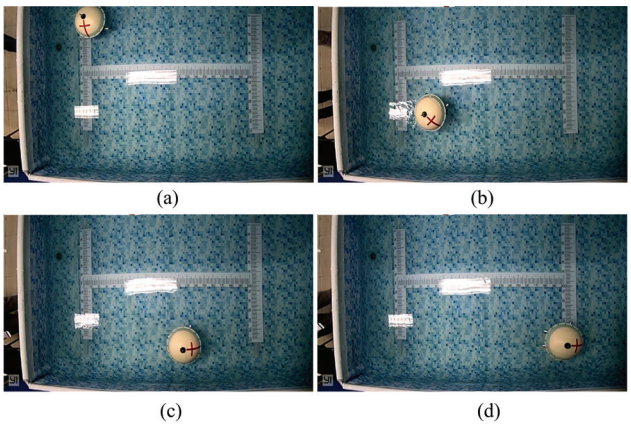

Fig. 10 Fuzzy PID-based turn bow motion experiment. (a) 0 s; (b) 8 s; (c) 12 s; (d) 16 s.

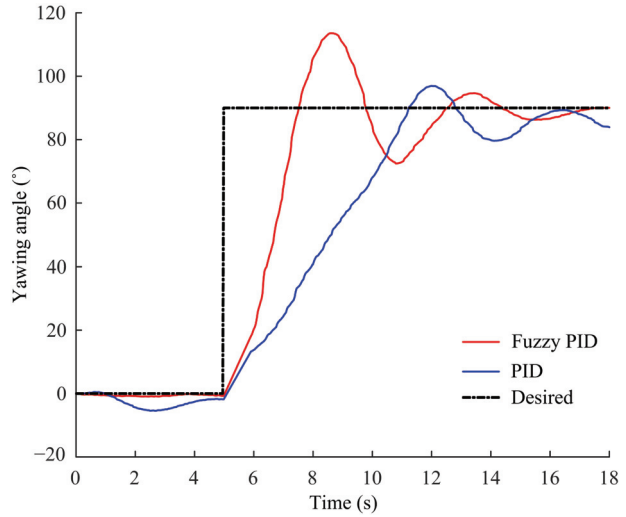

Fig. 11 Fuzzy PID and PID algorithms for turn bow motion: comparison of the experimental results.

the robot completed the underwater 3D motion experiments shown in Figs. 12a – 12i in approximately 37 s. Fig. 13 shows a video image captured by a camera in the water during the period when the images shown in Fig. 12 were captured.

Fig. 14 shows the relationship between the underwater 3D motion of the spherical amphibious robot, the time-heading angle diagram and the fuzzy PID control algorithm under hydrostatic conditions. From Fig. 14, we can see that when the robot is in the red section, it moves in a line controlled by the fuzzy PID algorithm at a constant depth, and then turns after traveling a certain distance. The black section shows the expected value of the heading angle, and the blue section shows the period when the robot was not subject to heading control. Thus, we can use this figure to determine the robot's heading when the depth is controlled.

Fig. 15 shows the time-depth relationship obtained when the robot was controlled by the fuzzy PID control algorithm under hydrostatic conditions. We can see that when the robot is in the blue section, it travels in a line at a constant depth, then turns and moves in a straight line again. The red section shows the heading of the robot when the robot is subject to depth control but without heading control. The black section shows the expected depth of the robot. Fig. 16 shows a 3D track result of time-heading angle-depth value diagram based on fuzzy PID control.

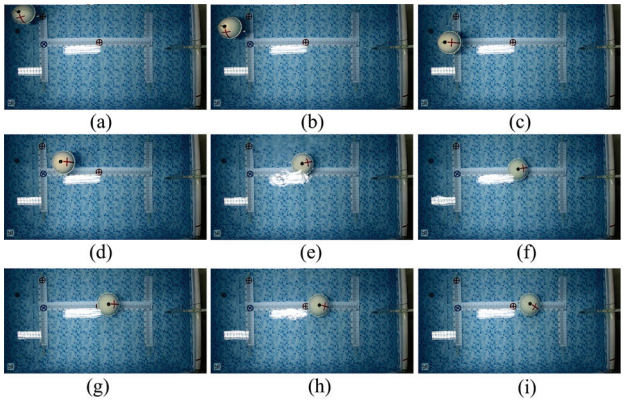

Fig. 12 3D motion experiment with fuzzy PID control (pool camera). (a) 0 s; (b) 4.5 s; (c) 9 s; (d) 13.5 s; (e) 18 s; (f) 22.5 s; (g) 27 s; (h) 31.5 s; (i) 37 s.

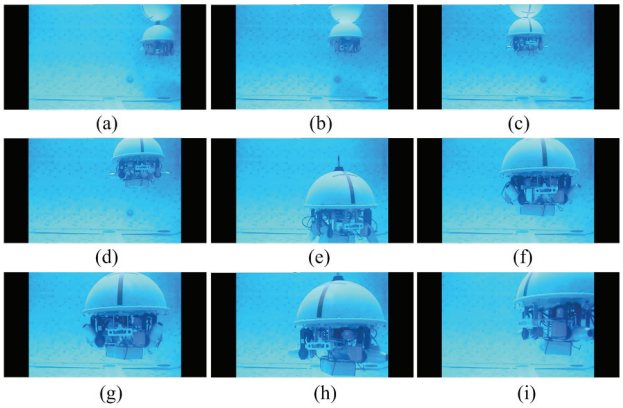

Fig. 13 3D motion experiment with fuzzy PID control (underwater camera). (a) 0 s; (b) 4.5 s; (c) 9 s; (d) 13.5 s; (e) 18 s; (f) 22.5 s; (g) 27 s; (h) 31.5 s; (i) 37 s.

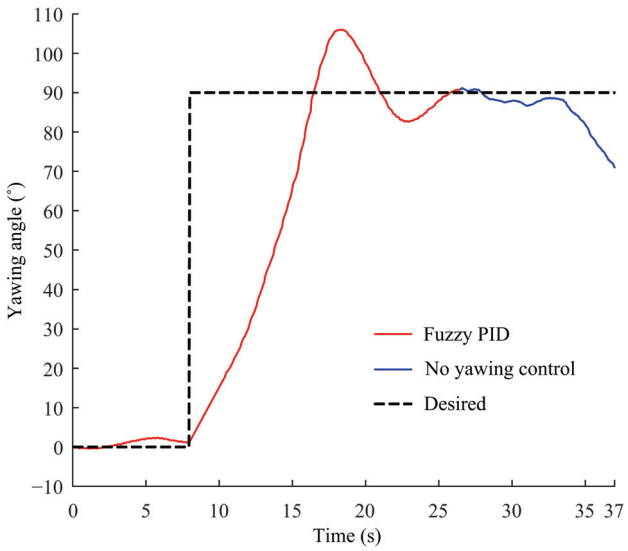

Fig. 14 Time-heading angle diagram obtained from the underwater 3D motion experiment with fuzzy PID control.

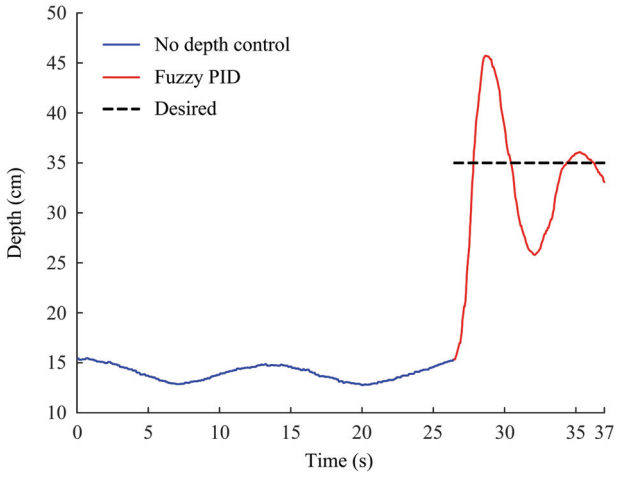

Fig. 15 3D motion experiment time-depth value diagram based on fuzzy PID control.

4 Conclusion

In this paper, to solve some problems of current amphibious robots and robot III, we improved the design of our amphibious spherical robot, developed a fourth-generation model and an underwater motion control system based on a fuzzy PID algorithm. The improvements to the design of the mechanical structure mainly involved driving mechanism and waterproof system. To solve the problems of heat dissipation issues and high power consumption, we redesigned the robot hardware circuit control system. Due to the real-time nature of the motion control system, we also developed an underwater motion control system based on a fuzzy PID algorithm to increase the motion control precision. We analyzed the kinematics and dynamics of the amphibious spherical robot by deriving a dynamic model of the robot. We then compared the forward and transition motions obtained using fuzzy and standard PID control algorithms, and validated the design of the underwater kinematic control system by carrying out experiments to characterize the rectangular motion, depth and underwater 3D motion control based on the fuzzy PID control algorithm. For the 3D motion, the robot moved in a straight line at a certain depth, then turned through a right angle. Once the robot reached a desired position, it dived towards a specified depth range. When the robot moves forward in a straight line, the maximum error of the PID control algorithm is approximately 8.45˚, while the maximum error of the fuzzy PID control algorithm is approximately 2.65˚. The mean square error is 0.8884˚ for the fuzzy PID control algorithm in this paper, while that is 10.8607˚ for the PID algorithms. The results of these experiments show that the fuzzy PID algorithm is more accurate and has better response characteristics than the standard algorithm.

Acknowledgment

This research was supported by National Natural Science Foundation of China (Nos. 61773064 and 61503028), National Key Research and Development Program of China (2017YFB1304404), and National Hightech Research and Development Program (863 Program) of China (No. 2015AA043202).

References

[1] Zhou Y C, Zhong B, Fang T, Liu J M, Zhou X N, Zhang S W. Application of bio-inspired control of AmphiHex-I in detection of *Oncomelania hupensis*, the amphibious snail intermediate host of *Schistosoma japonicum*. *Industrial Robot*: *An International Journal*, 2017, **44**, 242–250.

[2] Scaradozzi D, Sorbi L, Zoppini F, Gambogi P. Tools and techniques for underwater archaeological sites documentation. *Proceedings of OCEANS-San Diego*, San Diego, CA, USA, 2013, 1–6.

[3] Brown C J, Sameoto J A, Smith S J. Multiple methods, maps, and management applications: Purpose made seafloor maps in support of ocean management. *Journal of Sea Research*, 2012, **72**, 1–13.

[4] Zapata-Ramírez P A, Huete-Stauffer C, Scaradozzi D, Marconi M, Cerrano C. Testing methods to support management decisions in coralligenous and cave environments. A case study at Portofino MPA. *Marine environmental research*, 2016, **118**, 45–56.

[5] Dudek G, Giguere P, Prahacs C, Saunderson S, Sattar J, Torres-Mendez L A, Jenkin M, German A, Hogue A, Ripsman A, Zacher J, Milios E, Liu H, Zhang P F, Buehler M, Georgiades C. AQUA: An amphibious autonomous robot. *Computer*, 2007, **40**, 46–53.

[6] Honaryar A, Ghiasi M. Design of a bio-inspired hull shape for an AUV from hydrodynamic stability point of view through experiment and numerical analysis. *Journal of Bionic Engineering*, 2018, **15**, 950–959.

[7] Shi Q, Ishii H, Sugahara Y, Sugita H, Takanishi A, Huang Q, Fukuda T. Design and control of a biomimetic robotic rat for interaction with laboratory rats. *IEEE/ASME Transactions*

on Mechatronics, 2015, **20**, 1832–1842.

[8] Shi Q, Ishii H, Kinoshita S, Konno S, Takanishi A, Okabayashi S, Iida N, Kimura H, Shibata S. Modulation of rat behaviour by using a rat-like robot. *Bioinspiration & Biomimmetics*, 2013, **8**, 046002.

[9] Yu J Z, Wang M, Dong H F, Zhang Y L, Wu Z X. Motion control and motion coordination of bionic robotic fish: A review. *Journal of Bionic Engineering*, 2018, **15**, 579–598.

[10] Yu J Z, Chen S F, Wu Z X, Chen X Y, Wang M. Energy analysis of a CPG-controlled miniature robotic fish. *Journal of Bionic Engineering*, 2018, **15**, 260–269.

[11] Shi Q, Li C, Li K, Huang Q, Ishii H, Takanishi A, Fukuda T. A modified robotic rat to study rat-like pitch and yaw movements. *IEEE/ASME Transactions on Mechatronics*, 2018, **23**, 2448–2458.

[12] Gao Z H, Shi Q, Fukuda T, Li C, Huang Q. An overview of biomimetic robots with animal behaviors. *Neurocomputing*, 2019, **332**, 339–350.

[13] Boxerbaum A S, Oro J, Peterson G, Quinn R D. The latest generation Whegs™ robot features a passive-compliant body joint. *Proceedings of IEEE/RSJ International Conference on Intelligent Robots and Systems*, Nice, France, 2008, 1636–1641.

[14] Salumäe T, Raag R, Rebane J, Ernits A, Toming G, Ratas M, Kruusmaa M. Design principle of a biomimetic underwater robot U-CAT. *Proceedings of Oceans-St*, John's, St. John's, NL, Canada, 2014, 1–5.

[15] Yamada H, Chigisaki S, Mori M. Development of amphibious snake-like robot ACM-R5. *Proceedings of* 36*th International Symposium on Robotics*, Tokyo, Japan, 2005, 433–440.

[16] Georgiades C, German A, Hogue A, Liu H, Prahacs C, Ripsman A, Sim R, Torres L A, Zhang P F, Buehler M, Dudek G, Jenkin M, Milios E. AQUA: An aquatic walking robot. *Proceedings of IEEE/RSJ International Conference on Intelligent Robots and Systems*, Sendai, Japan, 2004, **4**, 3525–3531.

[17] Kaznov V, Seeman M. In outdoor navigation with a spherical amphibious robot. *Proceedings of IEEE/RSJ International Conference on Intelligent Robots and Systems* (*IROS*), 2010, Taipei, 5113–5118.

[18] Ye P, Sun H X, Qiu Z J, Chen J Z. Design and motion control of a spherical robot with stereovision. *Proceedings of IEEE* 11*th Conference on Industrial Electronics and Applications* (*ICIEA*), Hefei, China, 2016, 1276–1282.

[19] Yin X Y, Wang C W, Xie G M. A salamander-like amphibious robot: System and control design. *Proceedings of the International Conference on Mechatronics and Automation*, Chengdu, China, 2012, 956–961.

[20] Crespi A, Karakasiliotis K, Guignard A, Ijspeert A J. Salamandra robotica II: An amphibious robotto study salamander-like swimming and walking gaits. *IEEE Transactions on Robotics*, 2013, **29**, 308–320.

[21] Crespi A, Ijspeert A J. Salamandra robotica: A biologically inspired amphibious robot that swims and walks. In: Adamatzky A and Komosinski M eds., *Artificial Life Models in Hardware*, Springer, London, England, 2009, 35–64.

[22] Ding R, Yu J, Yang Q, Tan M. Dynamic modelling of a CPG-controlled amphibious biomimetic swimming robot. *International Journal of Advanced Robotic Systems*, 2013, **10**, 493–501.

[23] Zhang S W, Liang X, Xu L C, Xu M. Initial development of a novel amphibious robot with transformable fin-leg composite propulsion mechanisms. *Journal of Bionic Engineering*, 2013, **10**, 434–445.

[24] Cui L, Cheong P, Adams R, Johnson T. AmBot: A bio-inspired amphibious robot for monitoring the swan-canning estuary system. *Journal of Mechanical Design*, 2014, **136**, 115001–115001.

[25] Vogel A R, Kaipa K N, Krummel G M, Bruck H A, Gupta S K. Design of a compliance assisted quadrupedal amphibious robot. *Proceedings of the IEEE International Conference on Robotics and Automation* (*ICRA*), Hong Kong, China, 2014, 2378–2383.

[26] Kim H, Lee D, Liu Y, Jeong K, Seo T. Hexapedal robot for amphibious locomotion on ground and water. *Proceedings of the IEEE International Conference on Advanced Intelligent Mechatronics* (*AIM*), Busan, Korea, 2015, 121–126.

[27] Kim H, Lee D, Liu Y, Jeong K, Seo T. Hexapedal robotic platform for amphibious locomotion on ground and water surface. *Journal of Bionic Engineering*, 2016, **13**, 39–47.

[28] Scaradozzi D, Palmieri G, Costa D, Zingaretti S, Panebianco L, Ciuccoli N, Callegari M. UNIVPM BRAVe: A hybrid propulsion underwater research vehicle. *International Journal of Automation Technology*, 2017, **11**, 404–414.

[29] Watson S A, Green P N. Design considerations for micro-Autonomous Underwater Vehicles (*μ*AUVs). *Proceedings of* 4*th IEEE Conference on Robotics*, *Automation and Mechatronics* (*RAM*), Singapore, 2010, 429–434P.

[30] Watson S A, Crutchley D J P, Green P N. The design and technical challenges of a micro-autonomous underwater vehicle (μAUV). *Proceedings of IEEE International Conference on Mechatronics and Automation*, Beijing, China, 2011, 567–572P.

[31] Kaznov V, Seeman M. Outdoor Navigation with a Spherical Amphibious Robot. *Proceedings of the IEEE/RSJ International Conference on Intelligent Robots and Systems*, Taipei, Taiwan, 2010, 5113–5118.

[32] Satria S, Lee J W, Chan S. Portable amphibious spherical rolling robot with live-streaming capability for ground and aquatic deployment. *Proceedings of IRC Conference on Science*, *Engineering*, *and Technology*, Singapore, IRC, 2015, 1–4.

[33] Guo S X, Du J, Ye X F, Yan R, Gao H T. The computational design of a water jet propulsion spherical underwater vehicle. *Proceedings of IEEE International Conference on Mechatronics and Automation*, Beijing, China, 2011, 2375–2379.

[34] Guo S X, Du J, Lin X C, Yue C F. Adaptive fuzzy sliding mode control for spherical underwater robots. *Proceedings of IEEE International Conference on Mechatronics and Automation*, Chengdu, China, 2012, 1681–1685P.

[35] Shi L W, Guo S X, Mao S L, Yue C F, Li M X, Asaka K. Development of an amphibious turtle-inspired spherical mother robot. *Journal of Bionic Engeering*, 2013, **10**, 446–455.

[36] Guo S X, He Y L, Shi L W, Pan S W, Xiao R, Tang K, Guo P. Modeling and experimental evaluation of an improved amphibious robot with compact structure. *Robotics and Computer Integrated Manufacturing*, 2018, **51**, 37–52.

[37] Pan S W, Shi L W, Guo S X. A Kinect-based real-time compressive tracking prototype system for amphibious spherical robots. *Sensors*, 2015, **15**, 8232–8252.

[38] Guo S X, Pan S W, Shi L W, Guo P, He Y L, Tang K. Visual detection and tracking system for a spherical amphibious robot. *Sensors*, 2017, **17**, 870.

[39] He Y L, Shi L W, Guo S X, Pan S W, Wang Z. Preliminary mechanical analysis of an improved amphibious spherical father robot. *Microsystem Technologies*, 2016, **22**, 1–16.

[40] Guo S X, He Y L, Shi L W, Pan S W, Tang K, Xiao R, Guo P. Modal and fatigue analysis of critical components of an amphibious spherical robot. *Microsystem Technologies*, 2016, **23**, 1–15.

[41] Xing H M, Guo S X, Shi L W, He Y L, Su S X, Chen Z, Hou X H. Hybrid locomotion evaluation for a novel amphibious spherical robot. *Applied Sciences*, 2018, **8**, 156.

[42] Gu S X, Guo S X, Zheng L. A highly stable and efficient spherical underwater robot with hybrid propulsion devices. *Autonomous Robots*, 2020, **44**, 1–13.